Experimental Demonstration of an Optical-Label-Switching Router Architecture Supporting Selective 3R Regeneration

Zuqing Zhu, Bo Xiang, Haijun Yang, and S. J. Ben Yoo
Department of Electrical and Computer Engineering, University of California, Davis, California 95616, USA
Phone: (530)-752-7063, Fax: (530)-752-8428, Email: yoo@ece.ucdavis.edu

Abstract: We propose an optical-label-switching router architecture that utilizes selective-3R to offer regeneration in a smart and efficient way with only limited 3R capability. The experiment demonstrates error-free operation of selective-3R with all-optical burst-mode clock recovery.

OCIS codes: (060.4250) Networks, (060.4510) Optical Communications

1. Introduction

Optical-label-switching (OLS) is an attractive technology geared towards seamless integration of data and optical networking. Optical 3R regeneration re-amplifies, reshapes, and retimes the data payloads in OLS packets to extend the reach of the optical signal without repeated high-speed O/E/O conversions. However, in an optical network with reasonably good link characteristic, providing 3R regeneration at each hop is not necessary [1], but only greatly increases the router system complexity. In this paper, we propose an OLS router architecture that utilizes selective 3R to support 3R function in a more efficient way. Fig. 1 shows a simplified illustration of the proposed architecture. It is modified from our previous OLS router architecture in [2], and designates one input port as the 3R regeneration port. When a packet that requires 3R regeneration comes in, the switch controller will select it out by examining the label content and forward it to the 3R port through the loop-back fiber. One 3R line-card in the 3R port will then regenerate the payload and forward it to the desired output port. With this selective 3R scheme integrated, the OLS router only needs limited 3R capability to offer 3R regeneration in a smart and efficient way. In addition, another level of Quality-of-Service (QoS) control can be obtained with the selective 3R regeneration. In this paper, we experimentally demonstrate the proposed architecture in a 10 Gb/s OLS network testbed.

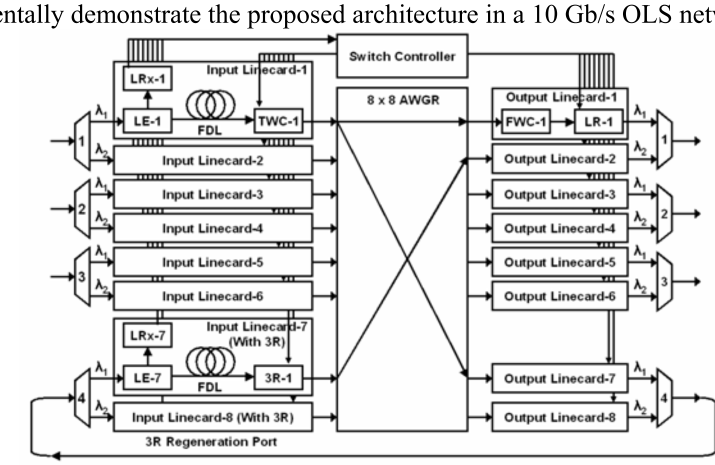

Fig. 1 Simplified architecture of an OLS router with limited 3R capability, LE: label extractor, LRx: label receiver, TWC: tunable wavelength converter, AWGR: arrayed waveguide grating router, FWC: fixed wavelength converter, LR: label rewriter.

2. Experimental Setup and Results

Fig. 2 shows the experimental setup that includes three OLS nodes and demonstrates selective, packetized 3R regeneration at Node 2. The insets of Fig. 2 show the detailed structures of building blocks of the OLS router. At Node 1, the subcarrier-multiplexed transmitter (SCM-Tx) in a two-arm configuration modulates 155 Mb/s labels and 10 Gb/s payloads separately before combining them into OLS packets [3]. The DFB laser diode (DFB) provides CW light at 1549.19 nm through a 50/50 fiber splitter. After mixing with a 14 GHz subcarrier, the label drives the $LiNbO_3$ modulator in the upper arm, generating a double-sideband optical SCM signal. The fiber Bragg grating (FBG) suppresses the optical carrier of the double-sideband SCM signal to avoid coherent crosstalk with the payloads [3]. In the lower arm, the two $LiNbO_3$ modulators (MODs) in cascaded operation generate payloads in the

©OSA 1-55752-830-6

return-to-zero (RZ) format. In the experiment, the SCM-Tx periodically generates OLS packets using payloads P1, P2, and P3 with different lengths: 9216, 8192, and 5120 bits, respectively. The OLS packets then experience 60 km large-effective-area-fiber (LEAF) transmission. The dispersion-compensation fiber (DCF) compensates for the chromatic dispersion of the fiber transmission. By adjusting the attenuator (ATT) after the DCF, we fix the optical-to-noise-ratio (OSNR) of the OLS packets as 26 dB at the input interface of Node 2. Fig. 3(b) shows the spectra of the OLS packets before (back-to-back) and after the LEAF fiber transmission. The label extractor (LE) utilizes FBG to separate the labels and the payloads all-optically [4]. The label burst-mode receiver (Bm-Rx) recovers the labels and forwards them to the switch controller for routing decisions. The tunable wavelength converter (TWC) is based on a tunable laser diode (TLD) and a semiconductor optical amplifier based Mach-Zehnder interferometer (SOA-MZI). The TWC takes the switching instruction from the switch controller and copies the payload onto a new wavelength that can direct it to the desired arrayed waveguide grating router (AWGR) output port. For a payload that is selected to go through 3R regeneration, however, the switch controller will direct it to the burst-mode 3R port. After 3R, the payload goes through AWGR again to its desired output port. The burst-mode 3R regenerator utilizes a SOA-MZI as the reshaping functional block. After reshaping, 50% power of the payload travels to the all-optical clock recovery block, where a combination of a Fabry-Perot filter (FPF) and a semiconductor optical amplifier (SOA) performs burst-mode clock recovery with amplitude equalization [5, 6]. The free spectrum range of the FPF is at 10 GHz to match to the payload data-rate, while the finesse is 100. The recovered clock is converted to electrical domain with the O/E converter and drives the optical modulator to retime the other 50% of the payload for reducing timing jitter [6]. After the switching fabric at Node 2, the payloads experience the second 50 km LEAF fiber transmission. The optical receiver located at Node 3 recovers the payloads for performance evaluation.

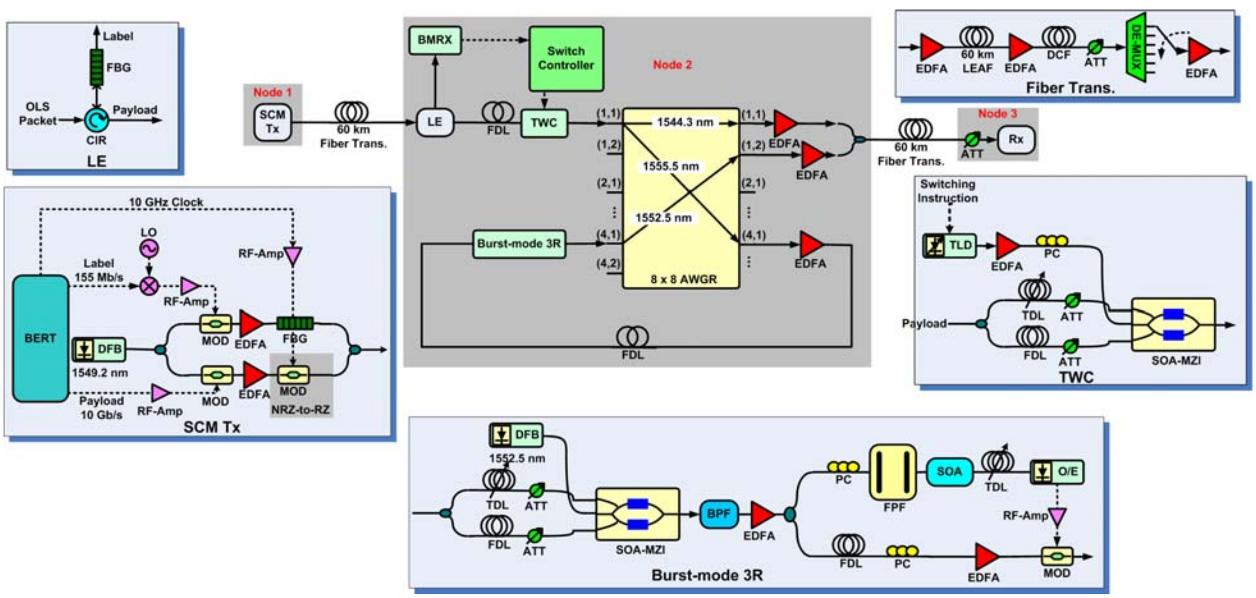

Fig. 2 Experimental Setup, BERT: Bit-error-tester, LO: Local oscillator, RF-amp: RF amplifier, EDFA: Erbium-doped fiber amplifier, CIR: Optical circulator, BMRX: Label burst-mode receiver, DE-MUX: De-multiplexer, PC: Polarization controller, TDL: Tunable delay line, FDL: Fixed delay line, BPF: Band-pass filter, O/E: Optical-to-electrical converter, Rx: optical receiver.

Fig. 3(a) shows the timing diagram and the oscilloscope screens of the payloads, demonstrating variable-length all-optical packet switching and selective burst-mode 3R regeneration. Here, $(m, n)_{IN}$ stands for n-th wavelength channel on the m-th input fiber, while a similar definition applies for output $(m, n)_{OUT}$. In the experiment, according to the label content, the switch controller picks P2 for burst-mode 3R regeneration, forwards it to the 3R port, and passes through P1 and P3. The oscilloscope screens in Fig. 3(a) show that the router produces the expected results. The oscilloscope screens also explain the timing relation between the clock and the data in the burst-mode 3R regenerator. The 20-80% rise time of the clock envelope is approximately 900 ps. The payload data stream is delayed 1 ns in the 3R regenerator to ensure being retimed with reasonably good clock. This delay does not affect the 3R at the packet tail for the reason that the recovered clock can maintain reasonably good amplitude (> 80% of the peak amplitude) for ~2 ns when the payload data is off. Fig. 3(c) shows the zoom-in screen of the recovered burst-mode clock. Fig. 3(d) shows the tunable laser output spectrum.

The payload bit-error-rate (BER) evaluation utilizes 2^{23}-1 pseudo-random-bit-sequence (PRBS). Fig. 4 shows the BER curves and the eye-diagrams. The curves marked as ‘after 1st Trans’ are measured before the TWC. The ‘after switching’ curves are for signals after the AWGR. The ‘after 2nd Trans’ curves are the final results for payloads at Node 3. The burst-mode 3R regeneration achieves ~1 dB negative penalty for P2 at 10^{-9} BER relative to that after the first fiber transmission. At the final output the BER curve for P1 and P3 is slightly bended due to noise accumulation, while the BER curve for P2 is still straight and achieves ~1 dB negative power penalty at 10^{-9} BER when comparing to P1 and P3. The eye-diagrams also show that signal of P2 after 3R has smaller timing jitter and clearer space- and mark-levels.

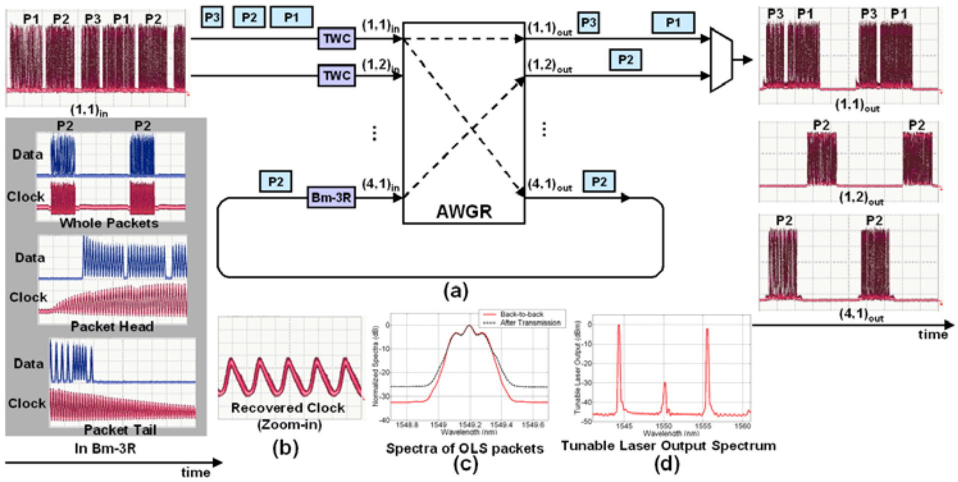

Fig. 3 (a) Timing diagram and the oscilloscope screens of the payloads, (b) Zoom-in screen of received burst-mode clock, (c) Spectra of OLS packets, (d) Tunable laser output spectrum

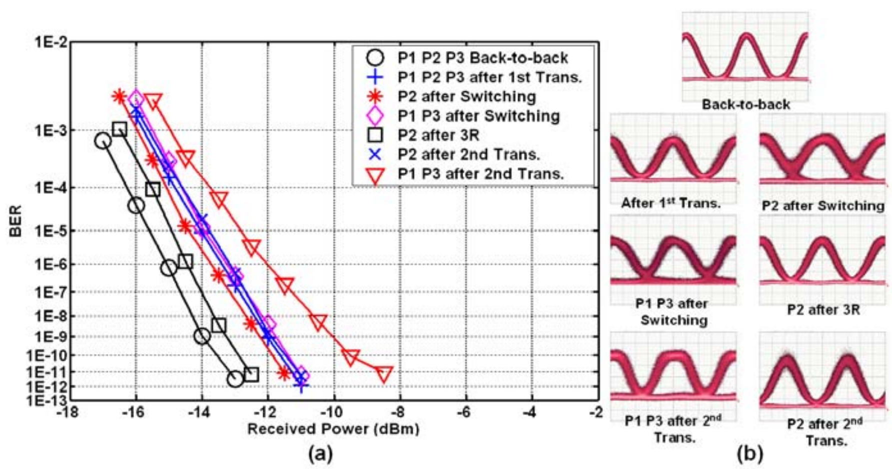

Fig. 4 Experimental results, (a) BER curves, (b) Eye-diagrams.

4. Summary

This paper proposed an OLS router architecture capable of selective packetized 3R regeneration. The architecture included a burst-mode 3R port to support 3R function in a limited, but efficient way. The experimental demonstration achieved error-free operation of the selective, packetized 3R regeneration employing all-optical burst-mode clock recovery in an OLS network testbed with fiber transmissions. The burst-mode 3R regeneration obtained ~1 dB negative power penalty at 10^{-9} BER.

5. References

[1] G. Gavioli, et al., *IEE Electron. Lett.*, vol. 41, pp. 146-148, Feb. 2005.
[2] F. Xue, et al., *J. Lightwave Technol.*, vol. 21, pp. 2595-2604, Nov. 2003.
[3] Z. Zhu, et al., *IEEE Photon. Technol. Lett.*, vol. 17, pp. 426-428, Feb. 2005.
[4] H. J. Lee, et al., *IEEE Photon. Technol. Lett.*, vol. 13, pp. 635-637, Jun. 2001.
[5] C. Bintjas, et al., *IEEE Photonics Technology Letters*, vol. 14, pp. 1363-5, Sept. 2002.
[6] Z. Zhu, et al., *IEEE Photon. Technol. Lett.*, vol. 18, pp. 718-720, Mar. 2006.